



UNIVERSITY
OF TRENTO

DIPARTIMENTO DI INGEGNERIA E SCIENZA DELL'INFORMAZIONE

38123 Povo – Trento (Italy), Via Sommarive 14
<http://www.disi.unitn.it>

A NUMERICAL APPROACH FOR THE EVALUATION OF THE
NONLINEAR EFFECTS ON THE ATTENUATION CONSTANT IN
HIGH TEMPERATURE SUPERCONDUCTION TRANSMISSION
LINES

S. Caorsi, M. Donelli, A. Massa, and M. Pastorino

December 2001

Technical Report # DISI-11-097

A numerical approach for the evaluation of the nonlinear effects on the attenuation constant in high temperature superconducting transmission lines.

S. Caorsi¹

Department of Electronics, University of Pavia, Pavia, Italy

M. Donelli, A. Massa, and M. Pastorino

Department of Biophysical and Electronic Engineering, University of Genoa, Genoa, Italy

Abstract. Superconducting materials exhibit an experimentally verified nonlinear dependence with respect to the magnetic field. In this paper, this nonlinearity is taken into account in the evaluation of the attenuation constant in propagating structures of practical usage. Quadratic and cubic nonlinearities are considered and an iterative numerical procedure is applied to calculate the attenuation constant. The nonlinearity in the penetration depth is also considered. In the results section, some typical structures are investigated. In particular, parallel-plane transmission lines filled by dielectric materials, microstrip lines, and striplines are considered. Comparisons with existing results show that this nonlinear behavior causes significant changes in the attenuation parameters.

1. Introduction

In the past years there has been a growing interest in superconducting materials and their applications. In particular, the discovery of high- T_c superconductors strongly changed the possibility of using these materials in the design of advanced devices for microwave electronics and other engineering applications [Van Duzer and Turner, 1981]. Since superconducting materials are characterized by a very small resistance, the design and realization of typical propagating structures (e.g. stripline, microstripline, etc.) by using these materials result in a great reduction of loss; in particular, the attenuation factors turn out to be some degrees lower comparing with those of normal conductors. For further developments in this area, it is necessary to accurately model the electromagnetic behaviour of high temperature superconducting (HTS) materials and, in particular, to devise methodologies for studying propagating structures which must be able to take into account this behaviour. In this respect, in the field of classical guided propagation, many efficient numerical approaches have been recently proposed. For example, a method to calculate the resistance and inductance of transmission lines with rectangular cross sections [Weeks *et al.*, 1991] is based on the network theory and permits to calculate the frequency-dependent resistance

¹Also at Department of Biophysical and Electronic Engineering, University of Genoa, Genoa Italy

and inductance per unit length matrices for transmission-line systems consisting of conductors with rectangular cross sections. The above method was extended in order to calculate resistance and inductance for a system of coupled superconducting transmission lines [Sheen *et al.*, 1991]. This goal has been accomplished by using the constitutive relation between the current density in the superconducting lines and the electric field, modeled by using the two fluid model. Nonlinear propagating structure have also widely numerically and experimentally studied (the reader can be referred to [Lee and Itoh 1989; El-Ghazaly *et al.* 1992; Oates *et al.*, 1991; Choudhury *et al.*, 1997] and references therein). Although most of the proposed approaches consider linear propagation only, nonlinear effects should be taken into account if the propagating structure have to operate under certain conditions [Van Duzer and Turner, 1981], in particular, when the magnetic field is high. The nonlinear effects were experimentally verified and further studied in several works [Oates *et al.*, 1991; Hein *et al.*, 1997; Ma and Wolff, 1996; Talanov *et al.*, 1999], in particular there has been a debate about the effective degree of nonlinearity, especially in the light of the recent improved film quality and depending of the patterned and unpatterned character of the film. In several papers, the nonlinear model was represented by a quadratic nonlinearity, whereas in other studies, different nonlinear behaviors were found to be suitable [Ma and Wolff, 1996 (a); Ma and Wolff, 1996 (b)], especially in the presence of high magnetic fields. A quadratic nonlinearity was also assumed in a computational approach [Caorsi *et al.*, 2001] devised for studying the interaction between an incident wave and a superconducting cylinder modeled by a negative permittivity. In the same paper, a preliminary result concerning the guided propagation has been reported with reference to the same degree of nonlinearity. In the present work, a numerical iterative procedure able to take into account the nonlinear effects on systems of multisuperconducting transmission line is presented. Since the main effect related to the nonlinearity with respect to the magnetic field is an increasing in the surface resistance of the superconductor, the present paper is focused on the evaluation of the attenuation constants of several guided structures of practical interest, for which the nonlinear behavior of the superconductors is rigorously taken into account and modeled by using some results derived from experimental data. The mathematical formulation starts from the two fluids model and is developed in the framework of the classic electrodynamics [Mei and Liang, 1991], which allows one to consider a superconducting material as a material with a complex conductivity σ_c . Dif-

ferent nonlinear behaviors (resulting from experimental analyses) can be easily incorporated into the model. In the following second- and third-order relations describing the nonlinearity versus the magnetic field are used and the results are compared. Moreover, the effects associated with changes in the penetration depth λ , due to the magnetic field, are taken into account, too. Although the rigorous treatment of the nonlinearity would involve the use of constitutive relationships written in terms of Volterra series [Censor, 1985; Censor, 1987], by using an approximation similar to the one involved in the so called distorted-wave Born approximation, an iterative approach for the computation of the attenuation factor is developed. Finally, some results are shown concerning guiding structures as parallel-plane transmission lines filled by dielectric materials, microstrip lines and striplines.

2. Mathematical Formulation

2.1. Parameters of a multiconductor transmission line system

Let us consider the propagating structure shown in Figure 1, which is constituted by $M + 1$ superconductors, one of them is used as reference and the others are used as signal lines. The cross section of each line is subdivided into segments and the current flowing into each segment is considered to be uniformly distributed over the cross section of the segment. The generic segment is indicated by n , whereas a segment of the reference conductor is chosen as reference and indexed as 0. In this segment flows the return current, which is the sum of all the currents in all the other N segments:

Figure 1.

$$i_{tot} = \sum_{j=1}^N i_j \quad (1)$$

By taking into account the nonlinearity with respect to the magnetic field, a nonlinear complex electric conductivity can be defined as follows:

$$\sigma_c^{nl}(H) = \sigma_{lin} + \mathcal{L}(H) \quad (2)$$

where $\mathcal{L}(H)$ is a nonlinear operator depending on the assumed model for the nonlinearity, σ_{lin} is the linear part of σ_c^{nl} , which, according to the two fluid model [Mei and Liang, 1991], can be expressed as

$$\sigma_{lin} = \sigma_1(T) - j \frac{1}{\omega \mu_0 \lambda^2(T)} \quad (3)$$

where ω is the angular frequency, μ_0 is the magnetic permeability, T is the temperature (K), and λ is the penetra-

tion depth of the superconductor. Each segment is characterized by a complex nonlinear resistance given by:

$$r_j^{nl}(H) = \frac{1}{\sigma_{c_j}^{nl}(H)A_j} \quad (4)$$

where the subscript j refers to the j -th segment of area A_j (cross section), and $\sigma_{c_j}^{nl}(H)$ is the nonlinear conductivity of the j -th segment (assumed to be constant). In this development we follow the approach described in [Weeks *et al.*, 1979] for normal conductors, and extended in [Sheen *et al.*, 1991] to deal with superconducting materials. In particular, a resistance matrix is constructed, whose elements are given by:

$$r_{jh}(H) = \text{Re} \left(\frac{1}{\sigma_{c_0}^{nl}(H)A_0} + \delta_{jh} \frac{1}{\sigma_{c_j}^{nl}(H)A_j} \right) \quad (5)$$

where h and j are the index of two generic segments, $\delta_{jh} = 1$ if $h = j$ and $\delta_{jh} = 0$ otherwise. Analogously, the inductance matrix is given by:

$$\begin{aligned} l_{jh}(H) &= l_{jh}^{(k)}(H) + (l_{jh} + l_{j0} + l_{0h} + l_{00})^{(m)} = \\ &= l_{jh}^{(k)}(H) + l_{jh}^{(m)} \end{aligned} \quad (6)$$

where $l_{hj}^{(k)}$ is the kinetic contribution given by:

$$l_{jh}^{(k)}(H) = \frac{1}{\omega} \text{Im} \left(\frac{1}{\sigma_{c_0}^{nl}(H)A_0} + \delta_{jh} \frac{1}{\sigma_{c_j}^{nl}(H)A_j} \right) \quad (7)$$

and the other terms l_{jh} can be computed as described in details in [Weeks *et al.*, 1979; Sheen *et al.*, 1991; Tsuk and Kong, 1991]. At this point, the impedance matrix $[z]$ of dimensions $N \times N$, whose elements are given by $z_{jh} = r_{jh}(H) + j\omega l_{jh}(H)$, is computed and inverted in order to obtain the admittance matrix $[y(H)] = [z(H)]^{-1}$. In this way, following [Sheen *et al.*, 1991], it is possible to compute the array containing the values of the current flowing in the segments, \underline{i} , and, finally, the matrix impedance of the transmission structure $[Z(H)]$ (dimensions $M \times M$). This matrix can be derived from the admittance matrix $[Y(H)]$, whose elements are given by:

$$Y_{mn}(H) = \sum_{j=N_{mi}}^{N_{mf}} \sum_{h=N_{ni}}^{N_{nf}} y_{jh}(H) \quad (8)$$

where N_{pi} and N_{pf} denote the first segment and the last segment of the p -th conductor, respectively; $y_{jh}(H)$ is the element of matrix $[y(H)]$. Finally, the attenuation constant can be computed by using the following relation in which the conductance is neglected:

$$\alpha^{nl}(H) = \text{Re}[\sqrt{(R(H) + j\omega L(H)) \cdot j\omega C(H)}] \quad (9)$$

where $R(H)$, $L(H)$ are the resistance and the inductance of the transmission line derived from the real and imaginary parts of the impedance matrix $[Z(H)]$, $C(H)$ is the capacitance derived as indicate in [Gupta *et al.*, 1979]. The computation is iteratively repeated, following an approach similar to the so-called distorted-wave Born approximation, which has been applied in [Caorsi *et al.*, 1993] to nonlinear dielectrics and detailed in [Caorsi *et al.*, 2001] for the computation of the interactions between an incident wave and a superconducting object. In particular at each iteration, the magnetic field is obtained on the basis of the current density of the previous step, starting by the linear case.

2.2. Choice of the nonlinear operator $\mathcal{L}(H)$

In order to apply the previously described method, a model for the \mathcal{L} operator must be employed. This model should result from experimental characterization of superconducting materials. According to the literature on the subject, two models are considered here.

2.2.1. Third-order nonlinearity Following the experimental data provided in [Oates *et al.*, 1991], a dependence of the surface resistance with respect to the microwave power is assumed. In particular, the following quadratic relation has been found to be a good approximation of this behavior:

$$R_s = R_{s0} + \alpha H^2 \quad (10)$$

where R_{s0} is the surface resistance for a very low H and α is a constant. From this relationship, one can deduce a quadratic nonlinearity for σ_1 and, consequently:

$$\mathcal{L}(H) = \beta H^2 \quad (11)$$

where

$$\beta = \frac{2\alpha}{\omega^2 \mu_0^2 \lambda^3} \quad (12)$$

The measurement was made in [Oates *et al.*, 1991] by considering a superconducting films made of $YBa_2Cu_3O_{7-x}$ at temperatures of 77K and 4K and for a frequency of 1.5 GHz. The value of α was found by using a numerical fitting based on a least-square approximation.

2.2.2. Second-order nonlinearity As mentioned in the previous section, in high-field regime, the quadratic relation used for approximating the surface resistance do not agree adequately with experimental results. In particular, it has been pointed out in [Ma and Wolff, 1996 (a); Ma and Wolff, 1996 (b)] that, when H is large, R_s increases faster than H^2 . In order to fit the experimental data provided in [Nguyen *et al.*, 1993] with a second-order

nonlinearity, a least-square fitting has been used. In particular, R_s has been modeled as follows:

$$R_s = R_{s0} + \alpha' H^3 + \beta' H^2 + \gamma H \quad (13)$$

The results are given in Figure 2 and described in Section 3. In the present case, we obtained:

Figure 2.

$$\mathcal{L}(H) = \eta H^3 + \theta H^2 + \tau H \quad (14)$$

where

$$\eta = \frac{2\alpha'}{\omega^2 \mu_0^2 \lambda^3} \quad (15)$$

$$\theta = \frac{2\beta'}{\omega^2 \mu_0^2 \lambda^3} \quad (16)$$

$$\tau = \frac{2\gamma}{\omega^2 \mu_0^2 \lambda^3} \quad (17)$$

In the following, for comparison purposes, we will use the experimental data in [Nguyen *et al.*, 1993] for a temperature of 4.3K and a frequency of 1.5 GHz. The superconducting material is a $YBa_2Cu_3O_{7-x}$, which has a critical temperature $T_c = 77K$.

2.2.3. Effects of the nonlinearity of λ on $\mathcal{L}(H)$ A more accurate model can be derived by taking into account the nonlinear effect of the magnetic field on the penetration depth λ , although this effect is usually negligible. Following the approach in [Oates *et al.*, 1991], the fractional change in penetration depth $\Delta\lambda/\lambda$, can be calculated as a function of the magnetic field H as:

$$\frac{\Delta\lambda}{\lambda} = \xi H^2 \quad (18)$$

Since $\frac{\Delta\lambda}{\lambda}$ has been found to be small, from the binomial approximation one can deduce the expression for the nonlinear operator $\mathcal{L}(H)$

$$\mathcal{L}(H) = \zeta H^2 + \chi H^4 \quad (19)$$

where

$$\zeta = \frac{2\alpha}{\omega^2 \mu_0^2 \lambda_0^3} \quad (20)$$

$$\chi = -\frac{6\alpha\xi}{\omega^2 \mu_0^2 \lambda_0^3} \quad (21)$$

3. Numerical examples

In this section, some guiding structures, commonly used in microwave applications, are considered and their attenuation constants are calculated by using the models

developed in the previous sections. The assumed structures (shown in Figure 3) are the following: (a) a stripline embedded in vacuum; (b) a microstrip; (c) a parallel-plane transmission line. The parameters adopted to characterize the third-order nonlinearity are those experimentally deduced in [Oates *et al.*, 1991]. Analogously, the parameters for the second-order nonlinearity are derived from [Nguyen *et al.*, 1993]. Figure 2 shows the comparison between these experimental data and the cubic function obtained by a least-square technique. In order to apply the numerical approach previously described, a nonuniform grid was superimposed to the cross section of each transmission line under examination. The grid cells are more concentrated in the central region of the return lines and near the edges of the signal line, where the current density is much greater. The smallest element of the grid has linear dimensions which are fractions of the penetration depth. In particular, this value was chosen equal to $\frac{\lambda}{4}$. In the first example, numerical results for the stripline configuration are reported. The width of the signal line of the stripline was $W_s = 150 \mu m$ and the widths of the ground planes were $W_{gd} = 8000 \mu m$, the distance between the two return lines was $d = 864 \mu m$ and the thickness of the superconductors was varied from $0.1 \mu m$ to $0.8 \mu m$. The structure is embedded in vacuum and is the same considered in [Sheen *et al.*, 1991], where a method to calculate the resistance, the inductance and the current distribution for a multisuperconductors transmission line was proposed. Figure 4, shows the values of the attenuation constant for the linear case, and for different values of the thickness of the superconductor. Figure 5 gives the same parameter versus the penetration depth, using the nonlinearity model proposed in Section 2.2.1. In particular, the following cases are considered: (a) $t = 0.1 \mu m$; (b) $t = 0.2 \mu m$; (c) $t = 0.3 \mu m$; (d) $t = 0.4 \mu m$; (e) $t = 0.8 \mu m$. The peak value of H is assumed in the range 25-500 Oe. It is worth notice that, for low values of the penetration depth, the attenuation constant is similar to that of the linear case and exhibits limited changes in the considered range of H values, for all the t considered. On the contrary, when the penetration depth increases, the effect of the nonlinearity is rather significant for all t . As expected, the attenuation constant decreases when the thickness of the superconductors increases.

Figure 6 shows the plot of the attenuation constant versus the penetration depth, which has been obtained by using the model described in Section 2.2.3. In particular, two values of t were assumed: (a) $t = 0.1 \mu m$ and (b) $t = 0.8 \mu m$. The differences between the results of Figure 5 and Figure 6 are very small (less than 0.1% for any λ and H). The nonlinearity of λ with respect to H is not very

Figure 3.

Figure 4.

Figure 5.

Figure 6.

significant on the attenuation constant. This confirms the considerations pointed out in [Oates *et al.*, 1991]. The nonlinearity effects on σ_1 are much more evident. Figure 7 shows the results for the second-order model (Section 2.2.2). In this case, too, we considered (a) $t = 0.1 \mu\text{m}$ and (b) $t = 0.8 \mu\text{m}$. As expected, the two models predict analogous results for low values of H , whereas for high H levels, notable changes can be noticed and the second-order nonlinearity predicts higher attenuation.

Figure 7.

In the second example, a microstrip line made of *YBCO* was considered (Figure 2 (b)). The dielectric substrate was made of *LaAlO₃* ($\epsilon_r = 25$) with a thickness $d = 500 \mu\text{m}$; the width of the signal line was $W_s = 150 \mu\text{m}$ and the width of the return line was $W_{gd} = 5000 \mu\text{m}$. The above structure is the same as considered in [Liu and Itoh, 1993]. The analysis is performed for different values of the thickness of the superconducting films in the range between $0.002 \mu\text{m}$ and $0.02 \mu\text{m}$. The results are provided in Figure 8 and correspond to those provided in [Liu and Itoh, 1993] (Figure 6). Figure 8 shows the values of the attenuation constant for different values of the films thickness, and the nonlinearity is modeled as described in Sections (a) 2.2.1 (quadratic nonlinearity), (b) 2.2.2 (cubic nonlinearity), and (c) 2.2.3 (nonlinearity of the penetration depth), for temperature values of 4K and 77K and assuming $\lambda(0)$ (linear) $= 0.22 \mu\text{m}$. As can be seen, for low H , the obtained values are in good agreement with those in [Liu and Itoh, 1993], which have been calculated in the linear case. In the third example, a parallel-plane transmission line (Figure 2 (c)) was considered. As in the previous examples, the superconductor used was *YBCO* and the dielectric substrate was made of *LaAlO₃* ($\epsilon_r = 25$). The thickness of the signal and return lines was $t = 0.1 \mu\text{m}$; the distance was $d = 0.1 \mu\text{m}$ and the widths of the superconductors were $W_{gd} = 150 \mu\text{m}$.

Figure 8.

Figure 9 shows the plots of the attenuation constant versus the penetration depth λ , using the models developed in Sections (a) 2.2.1, (b) 2.2.2. In order to have an idea of the differences in the behaviors predicted by the two models, Figure 10 shows the attenuation constant for different values of the penetration depth (in the range $0.1\text{-}1 \mu\text{m}$) and for two values of the peak H : (a) 25 Oe and (b) 500 Oe . When computed by using the nonlinear model in Section 2.2.3, very small differences (less than 0.05%), have been obtained with respect to the results reported in Figure 10 (a). Finally, the same configuration was analyzed, but assuming $t = 1 \mu\text{m}$ and $d = 1 \mu\text{m}$. The results are provided in Figure 11, where, for a consistency check, the values obtained by applying the analytical formulation in [Van Duzer and Turner, 1981] (linear case) are also reported.

Figure 9.

Figure 10.

Figure 11.

4. Conclusion

The attenuation constant of several superconducting transmission lines widely used in microwave applications has been calculated.

In particular, the experimentally-verified nonlinear behaviors of superconducting materials at microwave frequency has been taken into account. Quadratic and cubic expressions have been used to model the behavior of the superconducting material versus the magnetic field. The significant effect of the nonlinearity on the attenuation constant has been evaluated with reference to a number of configurations and propagation conditions. The importance of the modeling of the nonlinear effect clearly resulted from the reported computer simulations.

References

- Caorsi, S., A. Massa, and M. Pastorino, Iterative numerical computation of the electromagnetic fields inside weakly nonlinear infinite dielectric cylinders of arbitrary cross sections using the distorted-wave Born approximation, *IEEE Trans. Microwave Theory Tech*, 44, 3, 400-412, 1993.
- Caorsi, S., A. Massa, and M. Pastorino, Numerical Computation of the Interaction Between Electromagnetic Waves and Nonlinear Superconducting Materials, *IEEE Trans. Microwave Theory Tech.*, 2001, in press.
- Censor, D., Waveguide and cavity oscillations in the presence of nonlinear media, *IEEE Trans. Microwave Theory Tech.*, 33, 296-301, 1985.
- Censor, D., Harmonic and transient scattering from weakly nonlinear objects, *Radio Sci.* 22(2), 227-233, 1987.
- Choudhury, D. P., B. A. Willemsen, J. S. Derov, and S. Sridhar, Nonlinear response of HTSC thin film microwave resonators in an applied DC magnetic field, *IEEE Trans. Appl. Superconduct.*, 7, 1260-1263, 1997.
- El-Ghazaly, S., R. Hammond, and T. Itoh, Analysis of superconducting microwave structures: Application to microstrip lines, *IEEE Trans. Microwave Theory Tech.*, 40, 499-508, 1992.
- Gupta, K. C., R. Garg, and I. J. Bahl, *Microstrip lines and slotlines*, Norwood, MA: Artech House, 1979.
- Hein, M., et al., Fundamental limits of the linear microwave power response of epitaxial Y-Ba-Cu-O films, *IEEE Trans. Appl. Superconduct.*, 7, 1236-1239, 1997.
- Lee, L. H., S. M. Ali, and W. Gregory Lyons, Full-wave characterization of high T_c superconducting transmission lines, *IEEE Trans. Appl. Superconduct.*, 2, 49-57, 1992.

- Lee, H. Y., and T. Itoh, Phenomenological loss equivalence method for planar quasi-TEM transmission lines with a thin normal conductor or superconductor, *IEEE Trans. Microwave Theory Tech.*, 37, 1904-1909, 1989.
- Liu, Y., and Tatsuo I., Characterization of power-dependent high- T_c superconducting microstrip line by modified spectral domain method, *Radio Sci.*, 28, 913-918, 1993.
- Ma, J.-G., and I. Wolff, Electromagnetics in high- T_c superconductors, *IEEE Trans. Microwave Theory Tech.*, 44, 537-542, 1996.
- Ma, J.-G., and I. Wolff, Electromagnetic behaviour of high- T_c superconductors, *IEEE Trans. Magnetics.*, 32, 1160-1163, 1996.
- Mei, K. K., and G. Liang, Electromagnetics of superconductors, *IEEE Trans. Microwave Theory Tech.*, 39, 1522-1529, 1991.
- Nguyen, P. P., D. E. Oates, G. Dresselhaus, and M. S. Dresselhaus, Nonlinear surface impedance for $YBa_2Cu_3O_{7-x}$ thin films: Measurements and a coupled-grain model, *Phys. Rev. B*, vol. 48, 9, 6400-6412, 1993.
- Oates, D. E., A. C. Anderson, D. M. Sheen, and S. M. Ali, Stripline resonator measurement of Z_s versus H_{rf} in $YBa_2Cu_3O_{7-x}$ thin films, *IEEE Trans. Microwave Theory Tech.*, 39, 1522-1529, 1991.
- Sheen, D. M., Sami M. Ali, D. Oates, R. S. Withers and J. A. Kong, Current distribution, resistance, and inductance for superconducting strip transmission lines, *IEEE Trans. Appl. Superconduct.*, 1, 108-115, 1991.
- Talanov, V. V., L. V. Mercaldo, and S. M. Anlage, Measurement of the absolute penetration depth and surface resistance of superconductors using the variable spacing parallel plate resonator, *IEEE Trans. Appl. Superconduct.*, 9, 2179-2182, 1999.
- Tsuk, M. J., and J. A. Kong, A hybrid method for the calculation of the resistance and inductance of transmission lines with arbitrary cross sections, *IEEE Trans. Microwave Theory Tech.*, 39, 8, 1338-1347, 1991.
- Van Duzer, T., and C. W. Turner, *Principle of Superconductive Devices and Circuits*, New York: Elsevier, 1981.
- Weeks, W. T., L. L. Wu, M. F. McAllister, and A. Singh, "Resistive and inductive skin effect in rectangular conductors," *IBM J. Res. Develop.*, 23, 6, 652-660, 1979.
-

S. Caorsi, Dept. of Electronics, University of Pavia, Via Ferrata 1, 27100 Pavia Italy. (e-mail: caorsi@ele.unipv.it)

M. Donelli, A. Massa, and M. Pastorino, Department Biophysical and Electronic Engineering, University of Genoa, Via Opera Pia 11A, 16145 Genova Italy. (e-mail: donelli@dibe.unige.it; massa@dibe.unige.it; pastorino@dibe.unige.it)

(Received January 3, 2001; revised February 27, 2001; accepted March 31, 2001.)

Copyright 2001 by the American Geophysical Union.

Paper number 01RS2625.

0148-0227/98/98JA-00000\$09.00

Figure Captions

Figure 1. Problem geometry. Cross section of the multi-conducting transmission line.

Figure 1. Problem geometry. Cross section of the multiconducting transmission line.

Figure 2. Nonlinear surface resistance. Experimental data [Nguyen et al, 1993] and least-square fitting with a second-order nonlinearity (equation (13)).

Figure 2. Nonlinear surface resistance. Experimental data [Nguyen et al, 1993] and least-square fitting with a second-order nonlinearity (equation (13)).

Figure 3. Superconducting stripline (a), superconducting microstripline (b) and superconducting parallel-plate transmission line (c)

Figure 3. Superconducting stripline (a), superconducting microstripline (b) and superconducting parallel-plate transmission line (c)

Figure 4. Superconducting stripline. Attenuation constant versus the penetration depth λ for various film thickness t (linear case).

Figure 4. Superconducting stripline. Attenuation constant versus the penetration depth λ for various film thickness t (linear case).

Figure 5. Superconducting stripline. Attenuation constant versus the penetration depth λ for various peak values of H and various films thickness t : (a) $t = 0.1 \mu m$; (b) $t = 0.2 \mu m$; (c) $t = 0.3 \mu m$; (d) $t = 0.4 \mu m$; (e) $t = 0.8 \mu m$ (Quadratic nonlinearity (Section 2.2.1)).

Figure 5. Superconducting stripline. Attenuation constant versus the penetration depth λ for various peak values of H and various films thickness t : (a) $t = 0.1 \mu m$; (b) $t = 0.2 \mu m$; (c) $t = 0.3 \mu m$; (d) $t = 0.4 \mu m$; (e) $t = 0.8 \mu m$ (Quadratic nonlinearity (Section 2.2.1)).

Figure 6. Superconducting stripline. Attenuation constant versus the penetration depth λ for various peak values of H and various films thickness t : (a) $t = 0.1 \mu\text{m}$; (b) $t = 0.8 \mu\text{m}$ (Quadratic nonlinearity and nonlinearity in the penetration depth (Section 2.2.3)).

Figure 6. Superconducting stripline. Attenuation constant versus the penetration depth λ for various peak values of H and various films thickness t : (a) $t = 0.1 \mu\text{m}$; (b) $t = 0.8 \mu\text{m}$ (Quadratic nonlinearity and nonlinearity in the penetration depth (Section 2.2.3)).

Figure 7. Superconducting stripline. Attenuation constant versus the penetration depth λ for various peak values of H and various films thickness t : (a) $t = 0.1 \mu\text{m}$; (b) $t = 0.8 \mu\text{m}$ (Cubic nonlinearity (Section 2.2.2)).

Figure 7. Superconducting stripline. Attenuation constant versus the penetration depth λ for various peak values of H and various films thickness t : (a) $t = 0.1 \mu\text{m}$; (b) $t = 0.8 \mu\text{m}$ (Cubic nonlinearity (Section 2.2.2)).

Figure 8. Microstrip line. Normalized attenuation constant $\frac{\alpha}{\omega\sqrt{\mu_0\epsilon_0}}$ versus the films thickness t for various peak values of H and for temperature values of 4K and 77K. Nonlinear cases, modeled as in Sections (a) 2.2.1, (b) 2.2.2, (c) 2.2.3.

Figure 8. Microstrip line. Normalized attenuation constant $\frac{\alpha}{\omega\sqrt{\mu_0\epsilon_0}}$ versus the films thickness t for various peak values of H and for temperature values of 4K and 77K. Nonlinear cases, modeled as in Sections (a) 2.2.1, (b) 2.2.2, (c) 2.2.3.

Figure 9. Parallel-plane superconducting transmission line. Attenuation constant versus the penetration depth λ for various peak values of H . Films thickness $t = 0.1 \mu\text{m}$. (a) Quadratic and (b) cubic nonlinearities.

Figure 9. Parallel-plane superconducting transmission line. Attenuation constant versus the penetration depth λ for various peak values of H . Films thickness $t = 0.1 \mu\text{m}$. (a) Quadratic and (b) cubic nonlinearities.

Figure 10. Parallel-plane superconducting transmission line. Attenuation constant versus the penetration depth λ for the two nonlinear models considered (quadratic and cubic nonlinearities). Film thickness $t = 0.1 \mu\text{m}$. Peak values of H : (a) 25 Oe and (b) 500 Oe.

Figure 10. Parallel-plane superconducting transmission line. Attenuation constant versus the penetration depth λ for the two nonlinear models considered (quadratic and cubic nonlinearities). Film thickness $t = 0.1 \mu\text{m}$. Peak values of H : (a) 25 Oe and (b) 500 Oe.

Figure 11. Parallel-plane superconducting transmission line. Attenuation constant versus the penetration depth λ for various peak values of H . Films thickness $t = 1\mu m$. (a) Quadratic and (b) cubic nonlinearities.

Figure 11. Parallel-plane superconducting transmission line. Attenuation constant versus the penetration depth λ for various peak values of H . Films thickness $t = 1\mu m$. (a) Quadratic and (b) cubic nonlinearities.

Figures

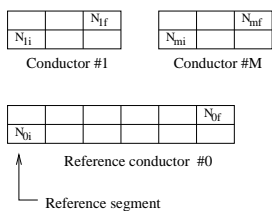


Figure 1. Problem geometry. Cross section of the multi-conducting transmission line.

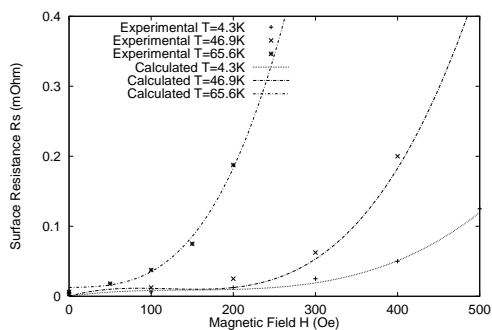


Figure 2. Nonlinear surface resistance. Experimental data [Nguyen et al, 1993] and least-square fitting with a second-order nonlinearity (equation (13)).

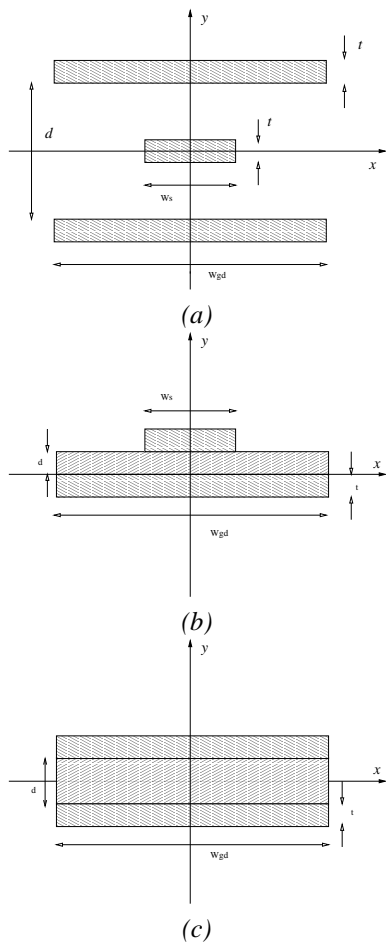


Figure 3. Superconducting stripline (a), superconducting microstripline (b) and superconducting parallel-plate transmission line (c)

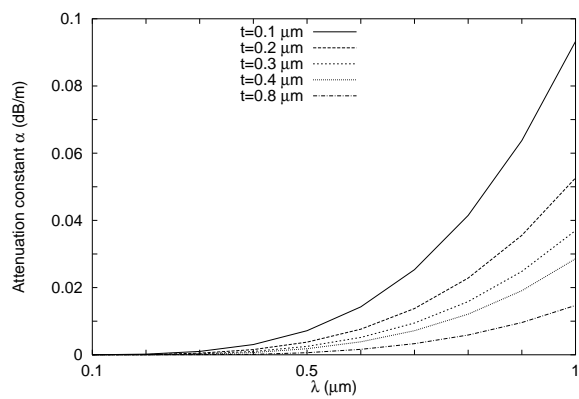


Figure 4. Superconducting stripline. Attenuation constant versus the penetration depth λ for various film thickness t (linear case).

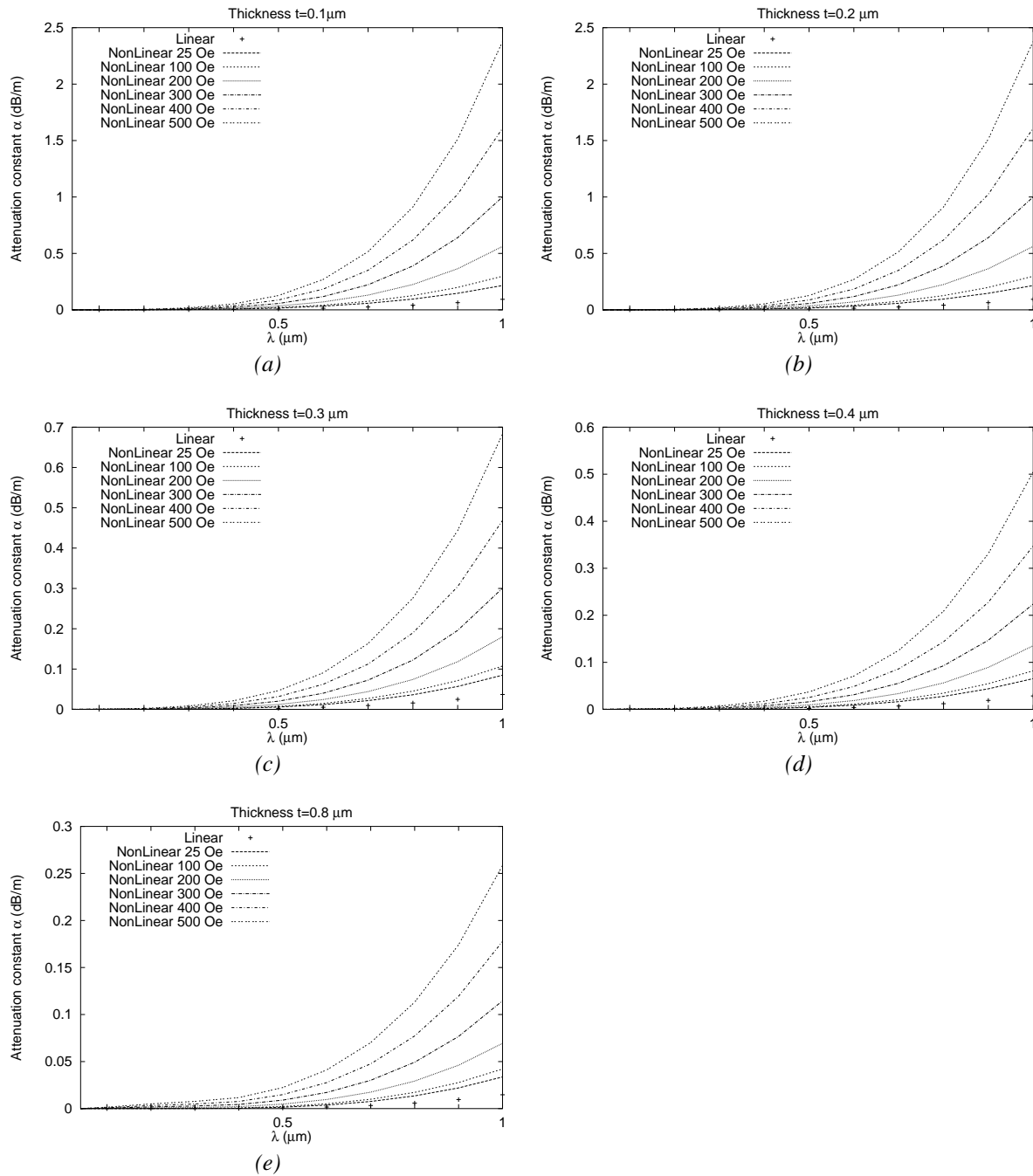


Figure 5. Superconducting stripline. Attenuation constant versus the penetration depth λ for various peak values of H and various films thickness t : (a) $t = 0.1 \mu\text{m}$; (b) $t = 0.2 \mu\text{m}$; (c) $t = 0.3 \mu\text{m}$; (d) $t = 0.4 \mu\text{m}$; (e) $t = 0.8 \mu\text{m}$ (Quadratic nonlinearity (Section 2.2.1)).

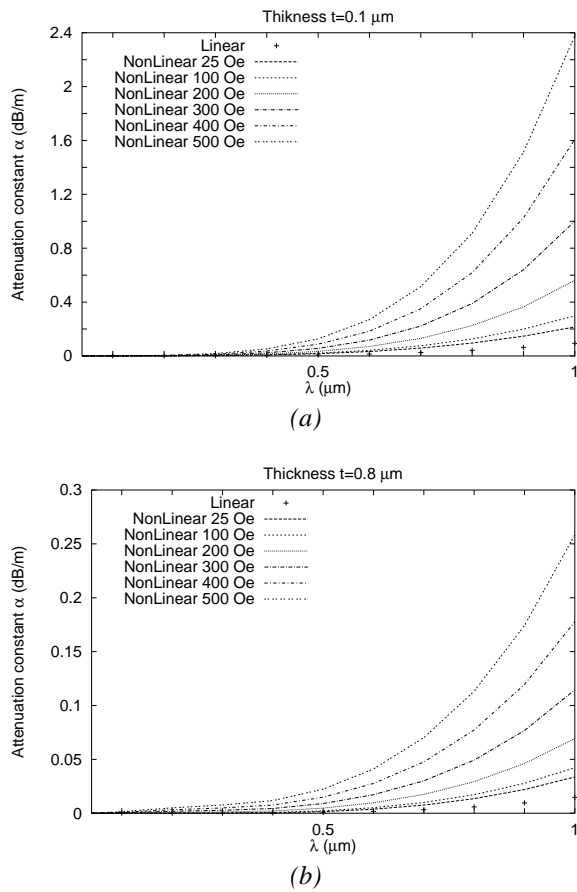


Figure 6. Superconducting stripline. Attenuation constant versus the penetration depth λ for various peak values of H and various films thickness t : (a) $t = 0.1 \mu\text{m}$; (b) $t = 0.8 \mu\text{m}$ (Quadratic nonlinearity and nonlinearity in the penetration depth (Section 2.2.3)).

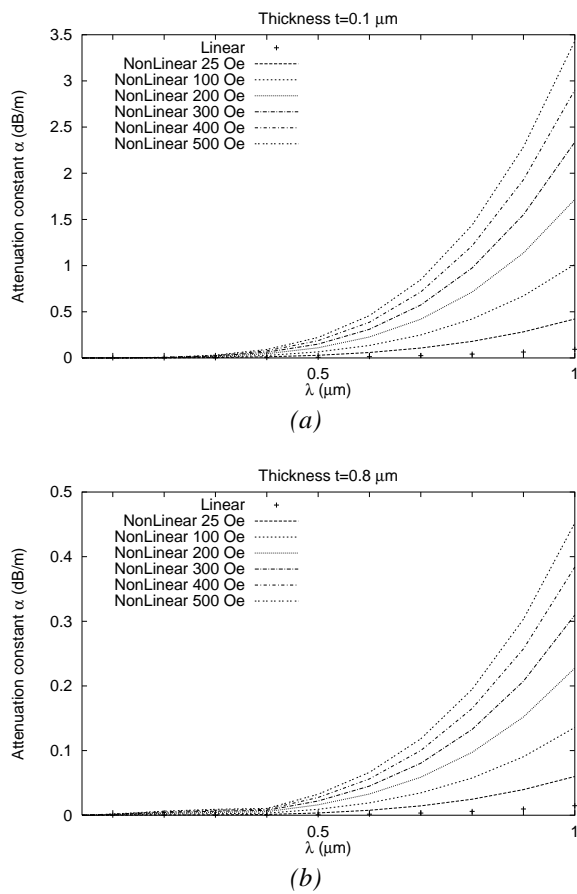
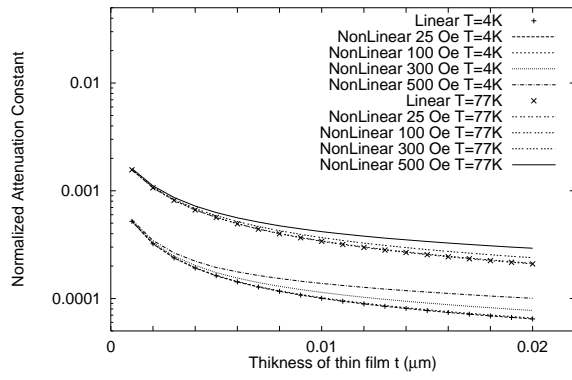
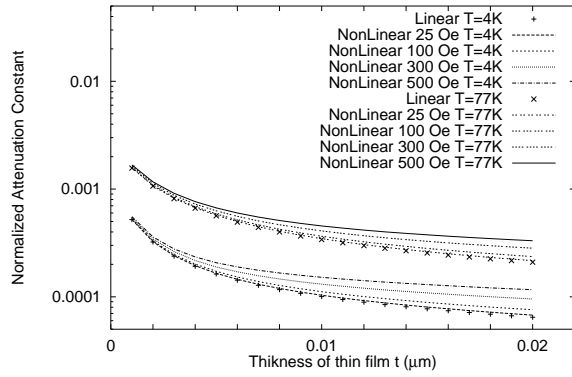


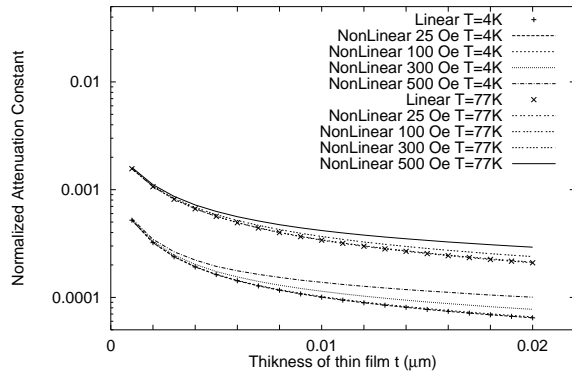
Figure 7. Superconducting stripline. Attenuation constant versus the penetration depth λ for various peak values of H and various films thickness t : (a) $t = 0.1 \mu\text{m}$; (b) $t = 0.8 \mu\text{m}$ (Cubic nonlinearity (Section 2.2.2)).



(a)



(b)



(c)

Figure 8. Microstrip line. Normalized attenuation constant $\frac{\alpha}{\omega\sqrt{\mu_0\epsilon_0}}$ versus the films thickness t for various peak values of H and for temperature values of 4K and 77K. Nonlinear cases, modeled as in Sections (a) 2.2.1, (b) 2.2.2, (c) 2.2.3.

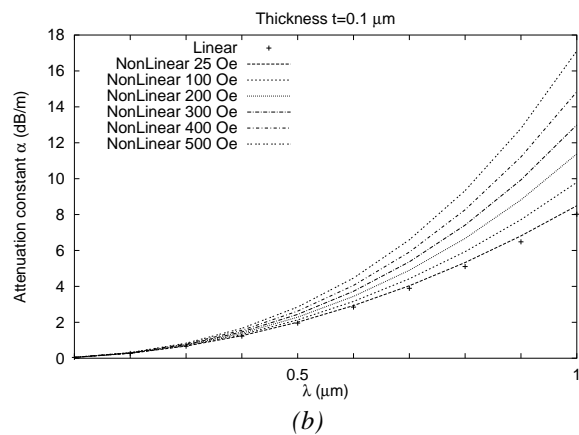
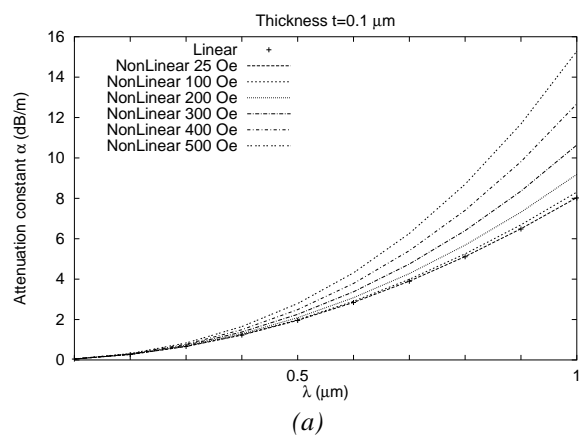


Figure 9. Parallel-plane superconducting transmission line. Attenuation constant versus the penetration depth λ for various peak values of H . Films thickness $t = 0.1 \mu\text{m}$. (a) Quadratic and (b) cubic nonlinearities.

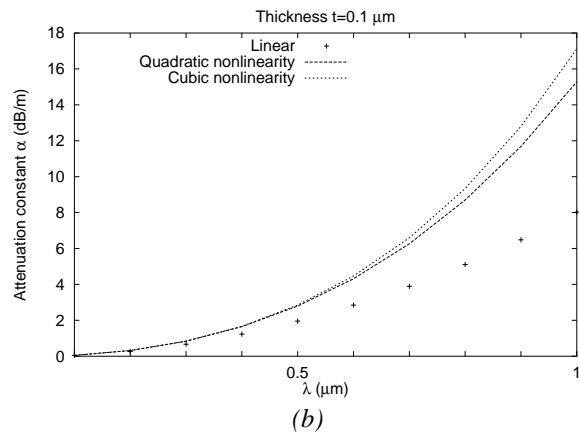
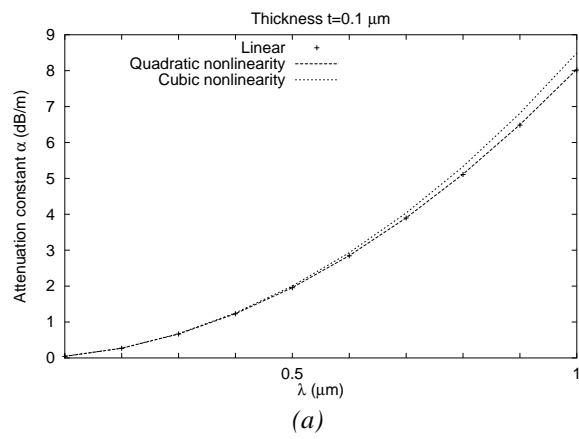


Figure 10. Parallel-plane superconducting transmission line. Attenuation constant versus the penetration depth λ for the two nonlinear models considered (quadratic and cubic nonlinearities). Film thickness $t = 0.1 \mu\text{m}$. Peak values of H : (a) 25 Oe and (b) 500 Oe.

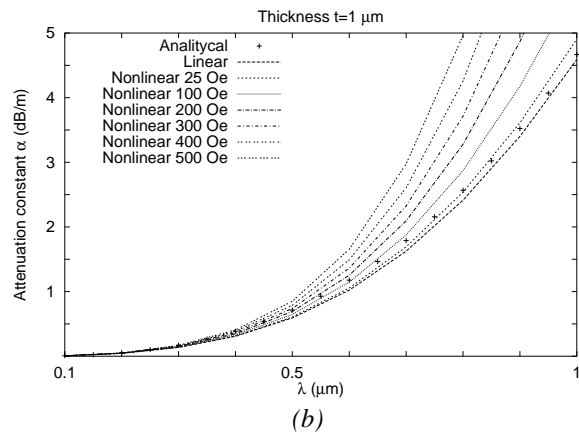
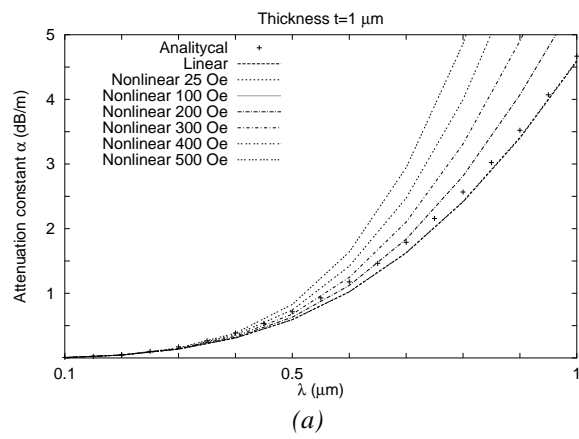


Figure 11. Parallel-plane superconducting transmission line. Attenuation constant versus the penetration depth λ for various peak values of H . Films thickness $t = 1 \mu\text{m}$. (a) Quadratic and (b) cubic nonlinearities.